**Journal Name**

Journal of Materials Chemistry B

Dynamic Article Links ▶

**ARTICLE TYPE**

# Designing the ordered micropatterned hydroxyapatite bioceramics to promote the growth and osteogenic differentiation of bone marrow stromal cells

**Cancan Zhao,[‡ab] Lunguo Xia,[‡c] Dong Zhai,[a] Na Zhang,[ab] Jiaqiang Liu,[c] Bing Fang,[c*] Jiang Chang[a*] and**
5 **Kaili Lin[a*]**

Patterned structured surfaces are very useful to control cell microenvironment and modulate cellular response, such as cell adhesion, migration, proliferation and differentiation. Herein, the ordered
10 micropatterns constructed by quadrate convex with different sizes were fabricated on hydroxyapatite [$Ca_{10}(PO_4)_6(OH)_2$, HAp] bioceramic surface using the ordered micropatterned nylon sieve as templates. The height, width and space of the convex for the patterns could be facilely regulated via simply tailoring the meshes of the template. Comparing with the traditional sample with flat surface, the fabricated HAp bioceramics with micropatterned surfaces possessed better wettability and higher surface energy, which
15 significantly promoted the adhesion, proliferation and osteogenic differentiation of rat bone marrow stromal cells (bMSCs). Furthermore, the pattern size close to that of the cell size showed better stimulation on cell response comparing with the larger pattern size. Our study suggested that the fabrication of the micropatterned structured HAp bioceramics is critical for designing the optimal biomaterials for bone regeneration and cell culture substrate applications.

## 20 1 Introduction

Many applications in stem cells highlight the important roles of the cell–material interactions in controlling cell functions.[1, 2] Thus, designing the materials to guide cell responses, and subsequently to stimulate the tissue formation has attracted great
25 attentions in biomaterial and tissue engineering fields, which is essential for the development of bioactive tissue regeneration materials.[3-7] In addition, it is well known that the cell behaviors are widely regulated by the chemical, structural and mechanical properties of the materials, etc.[5, 6, 8-10]

30 Previous studies suggested that fabrication of the material surface with microroughness,[11, 12] micro-/nano-structured topographies,[13-15] and patterned structured surfaces[1, 16, 17] can significantly improve the bioactivity and biological responses of the materials, and subsequently stimulate tissue regeneration
35 process. These essential roles of the surface topographies have been highlighted to modulate the cell behaviors.[18] Especially, comparing with the flat surface and unordered roughness surface,[19] the recent studies have confirmed that the biomaterial surface with ordered patterns could correctly command the
40 biological cellular responses, such as the cell shape, adhesion, cytoskeleton organization, spreading, migration and differentiation, etc.[18, 20-22] For example, previous studies have confirmed that the patterned surfaces can induce nucleolus morphology and reformation of cytoskeleton, and then direct the
45 preferential orientation of cells.[22-24] Most importantly, recent studies even found that the patterned structures could direct the

stem cells into functional characteristics by manipulating cell shape, orientation and migration.[25] Using conventional photolithography technique, Yang et al. developed a
50 hierarchically patterned structure consisted of microgroove structures incorporated with block copolymer nanopore patterns, which directed neural stem cells (NSC) differentiate into functional neurons, and subsequently potentiated NSC therapeutic efficacy.[18] Lee et al. reported the human embryonic
55 stem cells on the parallel ridge/groove pattern arrays fabricated by UV-assisted capillary force lithography could be facilely differentiated into neuronal lineage, which is useful for nerve injury repair.[26] Therefore, fabrication of ordered patterns on biomaterials is considered as an effective platform to induce
60 differentiation of stem cells towards specific lineages, which can be used to develop functional stem cell culture substrates and tissue engineered scaffolds for therapeutic applications.[26, 27]

Recently, some kinds of patterned structures have also been implemented on implant surfaces to improve their bioactivity and
65 tissue regeneration capacity.[8, 20, 28] Currently, the employed patterning methods mainly include lithography,[29, 30] mechanical punching and stenciling,[31] self-assembly,[32, 33] and chemical etching,[34] etc. Applying these methods, the patterns with parallel ridges and micro-groove,[22] pits or pillar,[35] dots,[20] array,[36] etc. on
70 the substrates of polymers, semi-conductors and metals have been widely fabricated. Up to now, it is still difficult to directly fabricate the patterns on bioceramic substrates due to their brittleness. The most commonly used methods for the fabrication of patterns on ceramic substrates include direct laser interference

patterning (DLIP) method,[37] micromachining technology,[38] and direct writing patterning process.[39] Berger et al. prepared periodic line- and cross-like patterns with 10 and 20 μm distances on hydroxyapatite [$Ca_{10}(PO_4)_6(OH)_2$, HAp] bioceramic surface using DLIP method.[37] The micromachining (e.g., microgrinding and micromilling) method has been widely applied to fabricate micropatterns on ceramic substrates. The microgrooves on zirconia and HAp ceramics with a minimum width of 100 μm have been fabricated by Holthaus et al. using micromachining method.[38] Chun et al. employed direct writing patterning process to deposit $Al_2O_3$ in line pattern with 200 μm width on many kinds of substrates.[39] However, most of these methods usually need complicated process and multi-steps, and special equipments. Moreover, the effect of micropatterns of bioceramics on biological responses, especially for the cell proliferation and osteogenic differentiation has rarely been studied, which play critical roles on the designing of tissue engineering materials and on the long-term success of the implants.

Therefore, it is urgent to develop a facile method for fabricating the patterned structured surfaces on bioceramics. In the present study, the ordered micropatterns were successfully constructed on the brittle substrate of HAp bioceramics using ordered nylon sieve as template. In particular, the pattern sizes could be facilely regulated via tailoring the meshes of the templates. Then the effect of the micropatterns on adhesion, proliferation and osteogenic differentiation of bone marrow stromal cells (bMSCs) was further investigated.

## 2 Materials and methods

### 2.1 Fabrication and characterization of HAp bioceramics with ordered micropatterns

HAp bioceramics with ordered micropatterned surfaces were fabricated by using a layer of ordered micropatterned nylon sieve as a template during the pressing of HAp nanoparticles. The HAp nanoparticles were synthesized by wet chemical precipitation method via reaction of $Ca(NO_3)_2 \cdot 4H_2O$ and $(NH_4)_2HPO_4$.[40] After calcination at 850 °C for 3 h, the obtained HAp powders were used as raw materials to fabricate HAp bioceramcis. The 6 wt.% polyvinyl alcohol was added into the HAp powders as binders. Then the mixtures were uniaxially compacted into pellets with a diameter of 10 mm and a thickness of 2.2 mm under a pressure of 8 MPa in a stainless steel die. To fabricate HAp bioceramics with micropatterned surface, the ordered nylon sieves with 100, 200 and 400 meshes were used as the templates (Fig. 1). In which, the templates with 10 mm diameter was first placed on the inner surface of the steel die, then the HAp powders was added and finally pressed into pellets. Subsequently, they were pressurelessly sintered in air at 1100 °C for 5 h at a heating rate of 2 °C/min, and then cooled to room temperature in the furnace. After sintering, the nylon templates could be completely burnt-out, and the HAp bioceramics with similar ordered micropatterns could be well duplicated from the templates. The fabricated HAp bioceramics with flat surface without using nylon sieve template were denoted as S0 for control sample, and the samples fabricated using 100, 200, and 400 mesh nylon sieves as templates were denoted as S1, S2, S3, respectively.

The surface morphologies and detailed structures of the fabricated samples were characterized by field emission scanning electron microscopy (FESEM: JSM-6700F, JEOL, Japan). The Olympus LEXT series of 3-dimensional (3D) measuring laser microscopes (LEXT: OLS4000, Olympus, Japan) with high-resolution and greater accuracy was applied to further observe the stereostructure of the micropatterns. Moreover, the height, width and space of the convex were determined from the laser microscopes. In addition, the surface roughness of the fabricated HAp bioceramics was evaluated by examining the amplitude parameter Sa and Sq using 3-dimensional (3D) measuring laser microscopes. In which, Sa is the arithmetic mean of the absolute departures of the roughness profile from the mean line throughout the sampling length, while the Sq is the root mean square deviation of the assessed profile. The surface hydrophilcity of the fabricated HAp bioceramics was characterized by measuring the contact angles using deionized water as medium on automatic contact angle meter (Kruss, Kruss GmbH Germany). Three samples from each group were analyzed to evaluate the average contact angle. The surface energy between pure water and air (72.8 mJ m$^{-2}$) was applied to calculate the surface energy of the samples based on the Girifalco−Good− Fowkes −Young rule.[11]

### 2.2 Isolation and culture of rat bone marrow stromal cells (bMSCs)

All animal procedures in vitro were approved by the Animal Research Committee of Shanghai 9th People's Hospital affiliated to Shanghai Jiao Tong University, School of Medicine. Fisher 344 rats were obtained from the Shanghai 9th People's Hospital Animal Center, and bMSCs were obtained and cultured as described in previous study.13 bMSCs were cultured in the Dulbecco's modified Eagle's medium (DMEM, Gibco, USA) with 10% FBS. Cultures were maintained at 37oC in a fully humidified atmosphere of 5% CO2 in air. The culture medium was changed after 24 h to remove non-adherent cells and then renewed three times a week until the primary mesenchymal cells reached 90 % confluence.13 Cells were passaged with the treatment of trypsin/EDTA (0.25% w/v trypsin, 0.02% EDTA). The cells were resuspended in fresh culture medium, and then seeded on the HAp bioeramics in 24-well tissue culture plates. A seeding density of 2×104 cells/well was used for studies on attachment, proliferation and osteogenic differentiation assays.

### 2.3 Morphology of the seeded bMSCs on patterned surface and flat HAp bioceramics

After being cultured for 6 h, the samples were taken out and rinsed with phosphate-buffered saline (PBS) two times to remove the nonadherent cells. The adherent cells were fixed in 4% paraformaldehyde for 30 min. Then the samples were treated with 0.1% Triton X-100 in PBS to permeabilize the cells for 20 min and then blocked with 1% BSA for 20 min. Finally, the actin cytoskeletons were labeled by incubating with Phalloidin- TRITC (Sigma, USA) for 30 min, while the cell nuclei were contrast-labeled in blue by 4',6-diamidino-2-phenylindole dihydrochloride (DAPI, Sigma, USA).[13] The actin cytoskeletons of cells were visualized with a confocal laser scanning microscope (CLSM, Leica, Germany).

In addition, after seeding the bMSCs on HAp bioceramics for 1 day, the samples were taken out and rinsed with PBS two times, then the samples were fixed in 2.5% glutaraldehyde overnight at 4 °C, washed three times with PBS for 5 min, dehydrated by increasing the concentration of ethanol (30, 50, 70, 90, 96 and 100%), and then dried using hexamethyldisilazane. Finally, the

samples were sputter-coated with gold and characterized by SEM (JSM-6700F, JEOL, Japan).
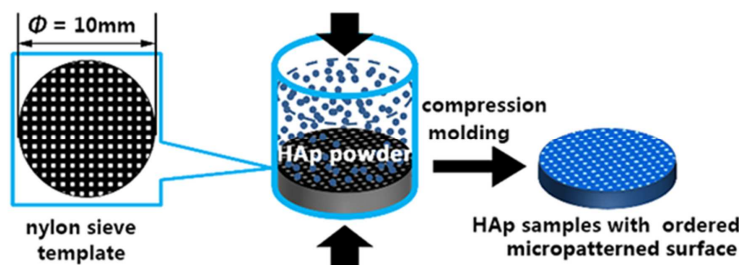


**Fig. 1.** Preparation scheme of HAp bioceramics with ordered micropatterned surface using nylon sieve as template.

### 2.4 Cell proliferation

To assay cell proliferation, the bMSCs were cultured on HAp bioceramic surfaces in 24-well plates for 1, 3 and 7 days. Three pieces of co-cultured discs for each group were washed twice with PBS to remove nonadherent cells. 300 μL of 3-(4,5-dimethylthiazol-2-yl)-2,5-diphenyl tetrazolium bromide (MTT, Amresco, USA) solution (0.5mg/mL) was added to each well for 2 h in the incubator under standard conditions. Then MTT solution was added and incubated at 37 $^{o}$C for 4 h to form MTT formazan. Finally, the medium was replaced with 300μL dimethyl sulfoxide (DMSO, Sigma, USA) in order to dissolve the formazan. The OD values were measured with ELX Ultra Microplate Reader (Bio-tek, USA) at 490 nm. All experiments were performed in triplicate.

### 2.5 Alkaline phosphatase (ALP) Activity Assay

According to the manufacturer's instruction (Beyotime, China), ALP staining was performed after bMSCs being cultured on flat HAp bioceramics (S0) and micropatterned HAp bioceramics (S1, S2, S3) for 10 days. Moreover, ALP activity was further quantified by measuring the transformation of p-nitrophenyl-phosphate (pNPP: Sigma, St. Louis, USA) into p-nitrophenol (pNP) after cell culture on S0-S3 for 4, 7 and 10 days.[13, 15] Briefly, the cells were dealt with trypsin/EDTA, followed by centrifuging, and then resuspended in lysis buffer with 0.2% pNP. Each sample was evenly mixed with 1 mg/mL pNPP in 1 M diethanolamine buffer and incubated at 37 °C for 15 min. The reaction was stopped by the addition of 3 N NaOH to the reaction mixture. Ultimately, ALP activity was quantified by measuring absorbance at 405 nm according to series of p-nitrophenol (pNP) standards.[15] When the total protein content was determined with the Bradford method in aliquots of the same samples with the Bio-Rad protein assay kit (Bio-Rad, Richmond, USA), read at 630 nm and calculated according to a series of BSA (Sigma) standards. The ALP activity was expressed as pNP (mM) per milligram of total cellular proteins.[15] All experiments were performed in triplicate.

### 2.6 Real-time PCR analysis

Total RNA was isolated from the cells cultured on flat HAp bioceramics (S0) and micropatterned HAp bioceramics (S1-S3) at days 4 and 7.[15, 41] At each time point, the cells were collected and resuspended in Trizol reagent (Invitrogen, USA). Each sample was reverse transcribed to cDNA using PrimeScriptTM RT Master Mix (TaKaRa, China). PCR reaction was performed using Ex Taq DNA polymerase (TaKaRa, China) for five genes:

Collagen 1 (COL1), osteocalcin (OCN), osteopontin (OPN), bone morphogenetic protein-2 (BMP-2), and Vascular endothelial growth factor (VEGF), while glyceraldehyde-3-phosphate dehydrogenase (GAPDH) was treated as the house-keeping gene for normalization. All experiments were performed in triplicate.

### 2.7 Statistical Analysis

All data were expressed as average ± standard deviation using ANOVA (SPSS, v.17.5, USA). The difference was considered statistically significant when $p < 0.05$.

## 3 Results

### 3.1 Fabrication and characterization of the micropatterns

Fig. 2 shows the surface topographies of the fabricated samples. It is clear to see that the highly ordered micropatterned structured surface on HAp bioceramics could be successfully duplicated from the structures of the nylon mesh (Fig. 2S1-S3). The micropatterns were constructed by near quadrate convex. In addition, the size and the space between the convex decreased apparently with the increase of the meshes of the nylon sieves. As expected, the sample with flat and mooth surface was obtained without using nylon sieve as template (Fig. 2S1). The topographies of the fabricated micropatterns were further characterized and confirmed using 3D laser measuring microscope (Fig. 3). The result showed that the values of Sa and Sq on micropatterned surfaces were larger than that on flat surface, which suggested that the surface roughness of the micropatterns was larger than that of the flat surface. In addition, the roughness decreased apparently with the decrease of the micropattern size. Moreover, the statistics data based on the 3D laser measuring results further confirmed that the height, width and space of the convex for the micropatterns decreased apparently with the increase of the meshes of the templates (Fig. 4), suggesting that the size of the micropatterns on HAp bioceramics could be well regulated by tailoring the meshes of the nylon sieve.
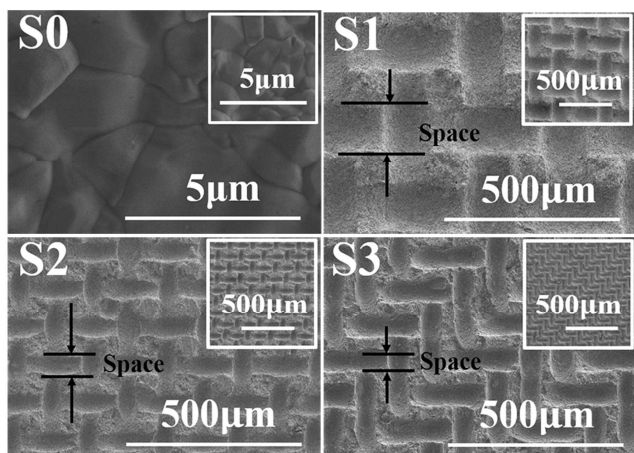
**Fig. 2.** FESEM images of the HAp bioceramic surfaces with flat surface (S0) as control sample, and the micropatterned surfaces using 100 (S1), 200 (S2) and 400 (S3) mesh nylon sieve as templates. The inserted small figures in top right corner were the low magnification images, and the mark of the "space" denote the distance between the adjacent convexes.
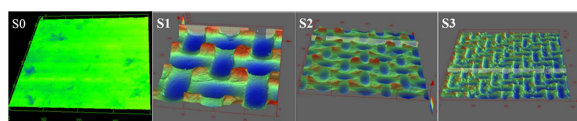


| | Sa(µm): | 0.364 ± 0.007 | 24.470 ± 0.303 | 7.832 ± 0.752 | 4.703 ± 0.312 |
| --- | --- | --- | --- | --- | --- |
| | Sq(µm): | 0.462 ± 0.008 | 30.252 ± 0.900 | 9.386 ± 0.726 | 5.533 ± 0.284 |

**Fig. 3.** 3D images and the surface roughness of the fabricated HAp bioceramic surfaces with flat surface (S0) as control sample, and the micropatterned surfaces using 100 (S1), 200 (S2) and 400 (S3) mesh nylon sieve as templates.
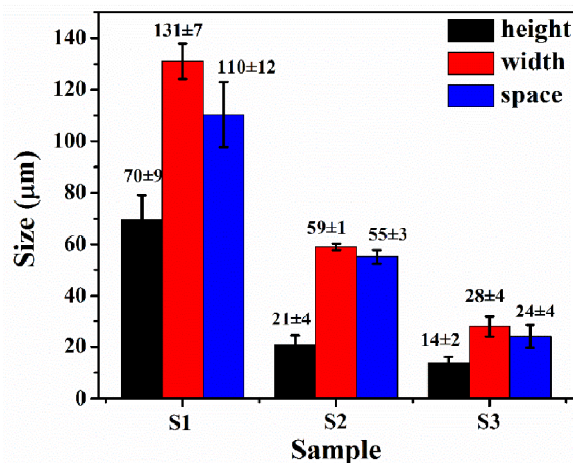


Fig. 4. The size of the height, width and space of the convex for the micropatterns fabricated using 100 (S1), 200 (S2) and 400 (S3) mesh nylon sieve as templates.

### 3.2 The effect of micropatterns on hydrophilicity and surface energy

Fig. 5 shows that the contact angle of the micropatterned surfaces (S1-S3) is smaller than that of the flat surface (S0), and the average values for the contact angle decreased apparently with the decrease of the micropattern size. The results suggested that the micropatterns apparently improve the hydrophilicity of the HAp bioceramics. In contrast, the surface energy of the micropatterned surfaces showed inverse tendency.
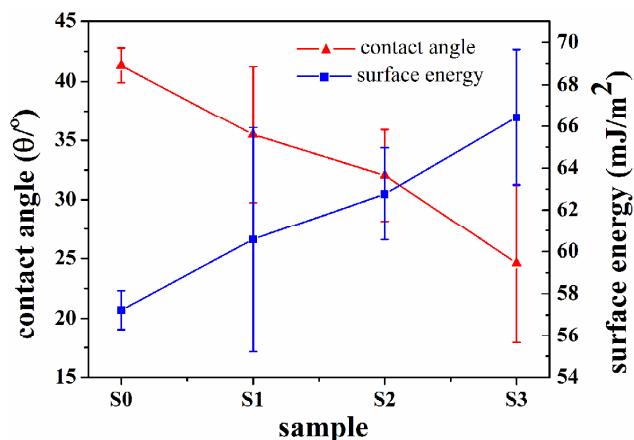


**Fig. 5.** Contact angle and surface energy of the samples with the flat surface (S0), and the micropatterned surfaces (S1-S3).

### 3.3 The effect of the micropatterns on adhesion and growth of the seeded bMSCs

Actin cytoskeletons were labeled to observe the cell morphology of seeded bMSCs after 6 h of being cultured on the fabricated HAp bioceramics S0–S3 (Fig. 6). Apparent differences in the cell morphology on the micropatterned HAp bioceramic (S1-S3) surfaces were found compared with the flat HAp sample. The cells attached on the HAp bioceramic with flat surface (S0) showed small size and almost in the absence of filopodia. On the contrary, the samples with micropatterned surfaces (S1-S3) especially for S3 enhanced the early cell attachment with apparent cytoplasmic extensions, and much more and longer actin filaments.
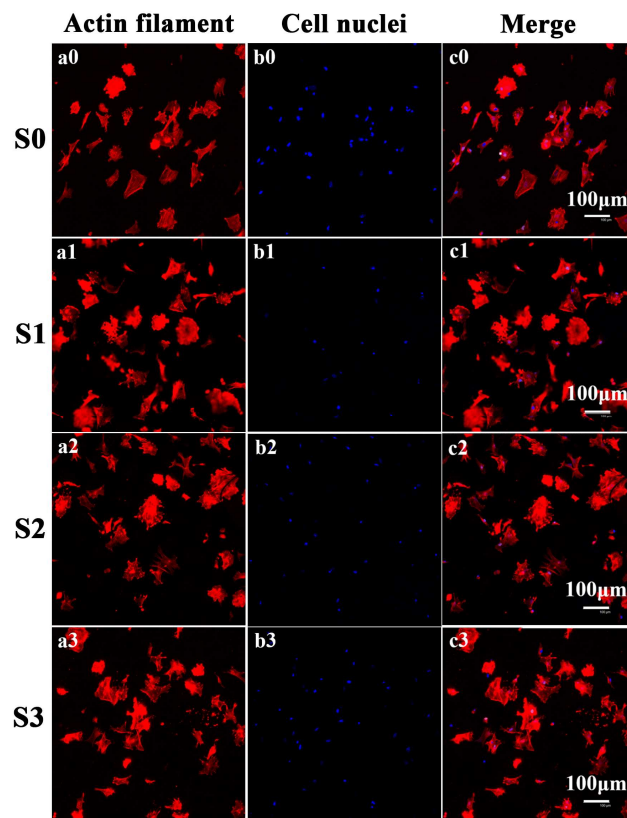


**Fig. 6.** Confocal microscopic images of the HAp bioceramics surfaces

with flat surface (S0) as control sample, and the micropatterned surfaces (S1-S3) after cells seeding for 6h.
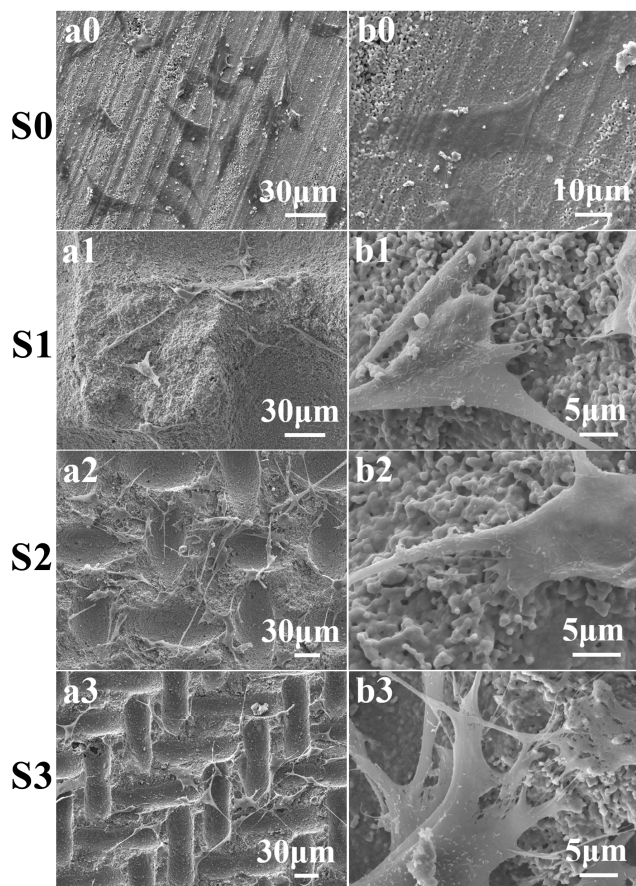


**Fig. 7.** SEM images of the HAp bioceramics surfaces with flat surface (S0) as control sample, and micropatterned surfaces (S1-S3) after cell seeding for 1 day. Fig. 7a0-a3 were the low magnification images, and those b0-b3 were high magnification images.

The SEM result was applied to further examine the effect of micropatterns on cell adhesion and morphology after 1 day of culture (Fig. 7). Obviously, the micropatterns still maintained better supporting on cell adhesions and spreading compared with the flat surface. It is clear to see that the cells adhesion on micropatterned surfaces (S1-S3) possess much more and longer filopodias compared with those on sample S0. Interestingly, the filopodias among the cells on micropatterned surfaces showed intertwined together (Fig. 7a1-a3), which was almost disappeared on flat surface (Fig. 7a0).

### 3.4 The effect of the micropatterns on the proliferation of bMSCs

The MTT assay was used to compare cell proliferation of bMSCs cultured on samples S0−S3 (Fig. 8). The results revealed that the amount of bMSCs increased apparently with the increase of the culture time on HAp bioceramic surfaces. In addition, the proliferation of bMSCs proceeded more significantly on micropatterned sample S1-S3 than that on flat sample S0. In addition, the sample S3 showed the highest stimulation on cell proliferation after 7 days of culture.
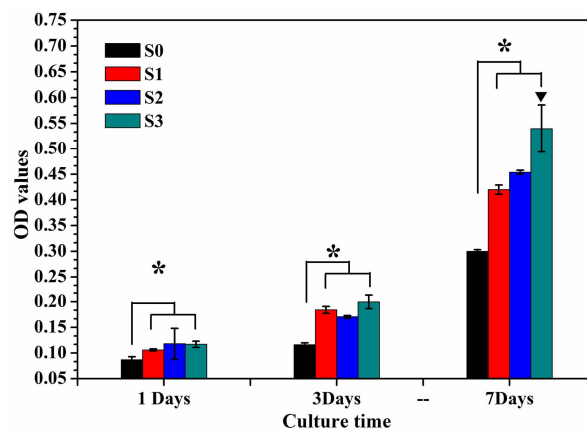


**Fig.8.** The proliferation of BMSCs cultured on control sample (S0), and the micropatterned samples (S1-S3) after seeding for 1, 3 and 7 days. (* significant differences between samples S0 and S1 ~ S3, ▼significant differences between samples S3 and S0 ~ S2, $p<0.05$).

### 3.5 The effect of the micropatterns on ALP activity of bMSCs

ALP staining was performed after bMSCs cultured on flat HAp bioceramics (S0) and the micropatterned HAp bioceramics (S1-S3) for 10 days (Fig. 9). As shown in Fig. 9A, the more intense ALP staining was found for cells cultured on micropatterned samples S1-S3, especially for S3, as compared with the cells cultured on sample S0. Furthermore, quantitative analysis revealed that the ALP activity for the cells cultured on patterned samples S1–S3 was higher than that on flat sample S0 at days 7 and 10, while there was only significant difference between samples S0 and S3 at days 4. In addition, the ALP activity increased apparently with the decrease of the micropattern size at days 10 (Fig. 9B).
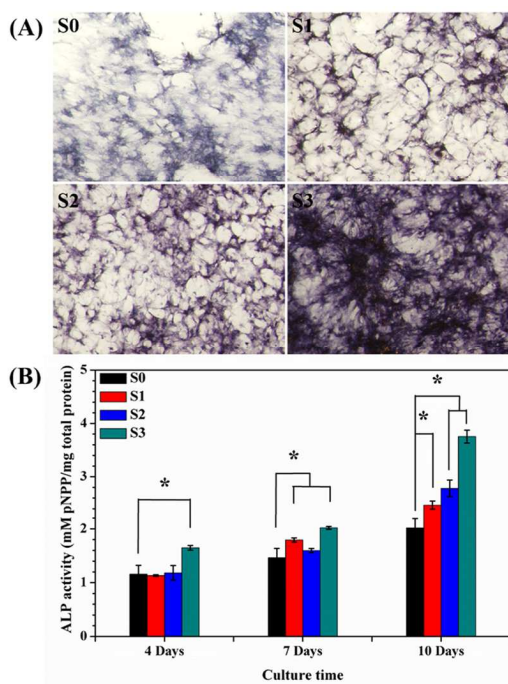


**Fig. 9.** ALP activity analysis: (A) ALP staining of bMSCs cultured on the flat sample (S0) and the micropatterned samples (S1-S3). (B) The quantitative results of ALP activity after seeding bMSCs on samples S0–S3 at days 4, 7 and 10. *$p < 0.05$.

### 3.6 The effect of the micropatterns on osteogenic differentiation of bMSCs

The expression level of the osteogenic genes including BMP-2, COLl, OCN, OPN and VEGF was examined by Real-time PCR after bMSCs cultured on samples S0-S3 for 4 and 7 days (Fig. 10). The results revealed that the constructed micropatterns could up-regulate the osteogenic differentiation of bMSCs at various degrees compared with the flat surface at days 4, except for BMP-2 and OPN on S2, and VEGF on S1. Increasing the culture time to days 7, the higher expression of these genes was almost maintained especially for sample S3.

## 4 Discussion

Compared with flat surface, the patterned structured surface can better stimulate or control the cellular responses and osteogenic expression of osteoblasts and bMSCs, which is very crucial for clinical applications. Most of the patterns on bioceramic surface
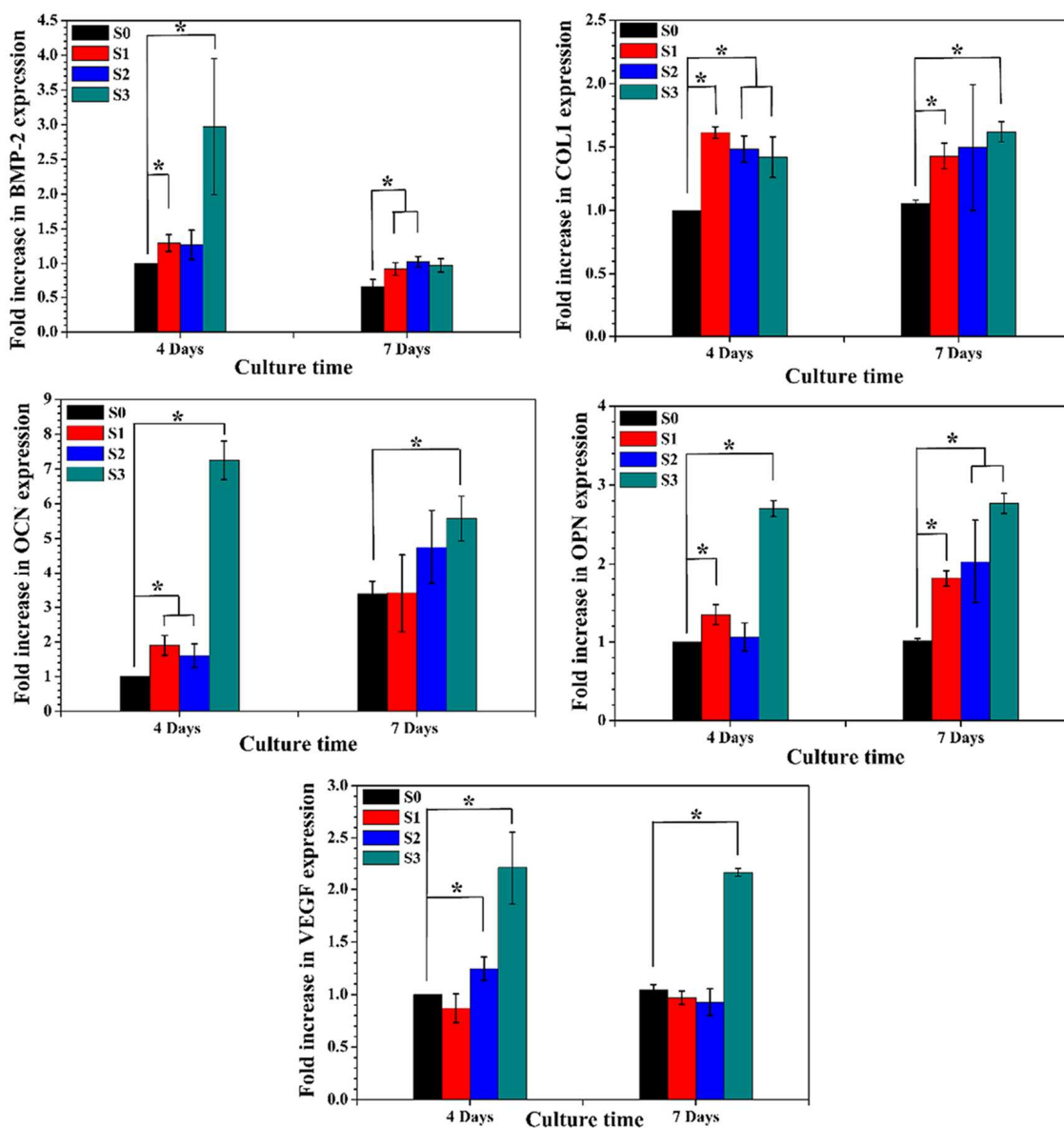


**Fig. 10.** Real-time PCR assay of bMSCs cultured on the flat sample (S0) and the micropatterned samples (S1-S3) at 4 and 7 days. *p < 0.05.

up to now were parallel ridges and grooves in microsize,[38] micro-array (eg. line-like pattern[37] and dimple[42]) etc. using the complicated and/or high-cost methods (eg. micromachining, laser interference ablation) due to the brittleness of bioceramics. It is still a great challenge to fabricate the ordered micropatterns on bioceramics in large-scale using simple and low-cost methods. In the present study, the ordered micropatterns constructed by near quadrate convex on HAp bioceramic surfaces were facilely created using ordered nylon sieve as template, and the template can be removed easily after calcination. In addition, the height and size of the convex as well as the convex space of the micropatterns could be facilely regulated by controlling the meshes of the nylon sieve.

Our results showed that the micropatterned HAp surfaces possessed superior wettability and surface energy (Fig. 5). Moreover, the hydrophilicity and surface energy increased with

the decrease of the micropattern size. In addition, as for the micropatterned samples, the decrease of the roughness could increase the wettability of the surfaces. Together with surface topography, it is considered that the increase of the initial hydrophilicity and surface energy may promote the early bone healing response at the cell−biomaterial interface via increasing the cell adhesion and consequently promotes response of mesenchymal stem cells (MSCs) and osteoblasts on the implant surfaces.[1, 15] Accordingly, the cell attachment assay in this study confirmed that the bMSCs attached and spread much better on micropatterned surfaces compared with the flat surface. The bMSCs on micropatterned HAp bioceramic surfaces showed much larger spreading areas, better cytoplasmic extensions, and much more and longer actin filaments comparing with the flat surface (Fig. 6 & 7). In addition, the apparent network formation among the adhesion cells on micropatterned surfaces was observed after 1 day of seeding (Fig. 7), which suggested that the cell-cell contact could be enhanced by micropatterned surfaces. Upon cell-cell contact, many surface molecules might conjugate with each other to form gap junctions, which might benefit for the subsequent cell responses such as better cell proliferation and differentiation.[43] The previous study of Sachar et al. showed that the gap junctions among cells can significantly promote the osteogenic and adipogenic differentiations of bMSCs.

Moreover, the constructed micropattern itself might possess better cell responses compared with flat surface. The previous studies highlighted that the patterned structures such as grooves, pits and posts, etc. could provide a good model for the three-dimensional (3D) in vivo environment to stimulate cell proliferation and differentiation in tissue engineering field.[3] In present study, the stimulation of cell proliferation and osteogenic differentiation was also found after culture of bMSCs on the fabricated HAp micropatterns with ordered convex structures (Fig. 8-10). As an early marker for osteogenic differentiation, ALP was crucial in regulating organic or inorganic phosphate metabolism via hydrolyzation of phosphate esters, and acts as a plasma membrane transporter for inorganic phosphates.[41] Compared with flat sample S0, there were about 22, 38, and 86% increase in ALP activity level of the cells cultured on micropatterned samples S1, S2 and S3 at 10 days, respectively (Fig. 9). Real-time PCR analysis of markers of BMP-2, COL1, OCN, OPN and VEGF was performed to further evaluate the effect of micropatterns on osteogenic differentiation (Fig. 10). BMP-2 is a potent osteoinductive cytokine, capable of inducing bone and cartilage formation in association with osteoconductive carriers such as collagen and synthetic HAp.[44] COL1 is known to be an early osteogenic marker and necessary for bone matrix formation, and OCN is considered as the major noncollagenous component related to bone matrix deposition and mineralization.[41] The OPN is associated with the maturation stage of osteoblasts during attachment and matrix synthesis before mineralization, and is largely considered as an intermediate or relatively earlier marker of osteogenic differentiation.[15] VEGF is a signal protein secreted by trabecular bone that stimulates vasculogenesis and angiogenesis.[45] The vasculogenesis and angiogenesis are extraordinarily important during bone regeneration, especially for critical sized bone defects.[46] However, the mechanism of promoted VEGF

expression initiated by micropatterns remains unknown, which needs to be further investigated in details. In this study, the higher expression level of BMP-2, COL1, OCN, OPN and VEGF on micropatterns at different degrees was observed. In addition, the sample S3 fabricated using 400 mesh nylon sieve as template showed the highest stimulation capacity. The highest osteogenetic differentiation of sample S3 may be due to the smaller micropatterned size, which was closer to cell size. The previous studies also revealed that the patterns with microgroove size close to or slightly smaller than that of the cell size could significantly stimulate the alignment and osteogenesis of bMSCs.[22, 47] Li et al. reported that the micropatterns with groove size of 25 μm could significantly enhance the elongation, spreading and proliferation of endothelial cells (ECs) in comparison with the flat surface or the samples with larger micropattern sizes.[48] In contrast, comparing with the micropatterned surfaces, most cells just adhered superficially on the flat surface at early stage.[47] Vasif et al. reported that bMSCs tend to adhere on flat surfaces instead of grooves when the groove width of the micropatterns was larger than 40 μm.[49] In the present study, the space of the convexs on micropatterned sample S3 is about 24 μm, which is close to the micropatterns with groove sizes of 25 μm reported by Li et al. Therefore, comparing with larger micropattern sizes, the sample S3 might possess the better stimulation ability on cell adhesion and spreading. Furthermore, the better cell adhesion increased the formation of focal contacts and filopodias, which enhanced the cell–cell interactions and ultimately promoted the cellular proliferation and differentiation.[43, 50]

Taken together with the adhesion, proliferation, and osteogenic differentiation studies, the HAp bioceramics with order micropatterned convex surfaces reported here might enhance osteoinductive ability via promoting bone formation directly in contact with the surface as well as in the surrounding tissue, which may provide an insight to future development of new bone implant materials. In addition, the micropatterned HAp bioceramics might be used as good substrate for the culture of osteoblasts and bMSCs, and the candidate as bone regeneration materials.

## 5 Conclusions

Designing the implants with patterned structures is considered as an effective method to stimulate the biological responses of biomaterials. In the present study, the HAp bioceramics with ordered micropatterned surfaces constructed by quadrate convex were facilely fabricated using nylon sieve as templateCompared with the flat surface, the fabricated micropatterns possessed better wettabilities and higher surface energies, and significantly stimulated the adhesion, spreading, proliferation and osteogenic differentiation of bMSCs. In addition, the micropattern size close to that of the cell size might possess better stimulation capacity. The results showed that the fabrication of micropatterned structures on materials might play an important role on the design of new bone implants, and the fabricated micropatterns can be used as excellent substrate to induce the biological responses.

## Acknowledgments

## Notes and references

*<sup>a</sup>State Key Laboratory of High Performance Ceramics and Superfine Microstructure, Shanghai Institute of Ceramics, Chinese Academy of Sciences, Shanghai 200050, China*
*<sup>b</sup>University of Chinese Academy of Sciences, Beijing 100049, China*
*<sup>c</sup>Center of Craniofacial Orthodontics, Department of Oral and Cranio-maxillofacial Science, Ninth People's Hospital Affiliated to Shanghai Jiao Tong University, School of Medicine, Shanghai 200011, China*
*‡ C.Z and L. X. are joint first authors.*
*Corresponding author: Fax: 86-21-52413903; Tel: 86-21-52412264. E-mail: lklsic@mail.sic.ac.cn (K. Lin); jchang@mail.sic.ac.cn (J. Chang); fangbing@sjtu.edu.cn (B. Fang)*

1. J. Kim, W. G. Bae, H. W. Choung, K. T. Lim, H. Seonwoo, H. E. Jeong, K. Y. Suh, N. L. Jeon, P. H. Choung and J. H. Chung, *Biomaterials*, 2014, 35, 9058-9067.
2. A. B. Faia Torres, S. Guimond Lischer, M. Rottmar, M. Charnley, T. Goren, K. Maniura Weber, N. D. Spencer, R. L. Reis, M. Textor and N. M. Neves, *Biomaterials*, 2014, 35, 9023-9032.
3. M. J. Poellmann, P. A. Harrell, W. P. King and A. J. Wagoner Johnson, *Acta biomaterialia*, 2010, 6, 3514-3523.
4. A. Higuchi, Q. D. Ling, Y. Chang, S. T. Hsu and A. Umezawa, *Chemical reviews*, 2013, 113, 3297-3328.
5. K. Lin, C. Wu and J. Chang, *Acta biomaterialia*, 2014, 10, 4071-4102.
6. W. Song, H. Lu, N. Kawazoe and G. Chen, *Langmuir*, 2011, 27, 6155-6162.
7. H. Jeon and G. Kim, *Journal of Materials Chemistry B*, 2014, 2, 171-180.
8. D. Wang, W. Zheng, Y. Xie, P. Gong, F. Zhao, B. Yuan, W. Ma, Y. Cui, W. Liu, Y. Sun, M. Piel, W. Zhang and X. Jiang, *Scientific reports*, 2014, 4, 6160.
9. Kumar G, Tison CK, Chatterjee K, Pine PS, McDaniel JH, Salit ML, Young MF and S. C. Jr., *Biomaterials*, 2011, 32, 9188–9196.
10. X. Yao, R. Peng and J. D. Ding, *Advanced Materials*, 2013, 25, 5257-5286.
11. J. W. Park, Y. J. Kim, C. H. Park, D. H. Lee, Y. G. Ko, J. H. Jang and C. S. Lee, *Acta biomaterialia*, 2009, 5, 3272-3280.
12. F. Gentile, L. Tirinato, E. Battista, F. Causa, C. Liberale, E. M. di Fabrizio and P. Decuzzi, *Biomaterials*, 2010, 31, 7205-7212.
13. L. Xia, K. Lin, X. Jiang, Y. Xu, M. Zhang, J. Chang and Z. Zhang, *Journal of Materials Chemistry B*, 2013, 1, 5403.
14. L. Xia, K. Lin, X. Jiang, B. Fang, Y. Xu, J. Liu, D. Zeng, M. Zhang, X. Zhang, J. Chang and Z. Zhang, *Biomaterials*, 2014, 35, 8514-8527.
15. K. Lin, L. Xia, J. Gan, Z. Zhang, H. Chen, X. Jiang and J. Chang, *ACS applied materials & interfaces*, 2013, 5, 8008-8017.
16. B. J. Papenburg, E. D. Rodrigues, M. Wessling and D. Stamatialis, *Soft Matter*, 2010, 6, 4377.
17. Z. Y. Qiu, C. Chen, X. M. Wang and I. S. Lee, *Regenerative Biomaterials*, 2014, 1, 67-79.
18. K. Yang, H. Jung, H. R. Lee, J. S. Lee, S. R. Kim, K. Y. Song, E. Cheong, J. Bang, S. G. Im and S. W. Cho, *ACS nano*, 2014, 8, 7809-7822.
19. M. Bigerelle, S. Giljean and K. Anselme, *Acta biomaterialia*, 2011, 7, 3302-3311.
20. M. S. Niepel, B. Fuhrmann, H. S. Leipner and T. Groth, *Langmuir*, 2013, 29, 13278-13290.
21. W. Song, X.L. Wang and G. P. Chen, *Soft Matter*, 2012, 8, 8429.
22. X. Shi, T. Fujie, A. Saito, S. Takeoka, Y. Hou, Y. Shu, M. Chen, H. Wu and A. Khademhosseini, *Advanced Materials*, 2014, 26, 3290-3296.
23. N. M. Alves, I. Pashkuleva, R. L. Reis and J. F. Mano, *Small*, 2010, 6, 2208-2220.
24. L. E. McNamara, R. Burchmore and M. O. Riehle, *Biomaterials*, 2012, 33, 2835-2847.
25. X. L. Wang, W. Song and G. P. Chen, *Soft Matter*, 2013, 9, 4160.
26. M. R. Lee, K. W. Kwon, H. Jung, H. N. Kim, K. Y. Suh, K. Kim and K. S. Kim, *Biomaterials*, 2010, 31, 4360-4366.
27. M. J. Kim, B. Lee, K. Yang, J. Park, S. Jeon, S. H. Um, D. I. Kim, S. G. Im and S. W. Cho, *Biomaterials*, 2013, 34, 7236-7246.
28. H. Li, Y. Xu, H. Xu and J. Chang, *Journal of Materials Chemistry B*, 2014, 2, 5492-5510.
29. H. Y. Chen, M. Hirtz, X. Deng, T. Laue, H. Fuchs and J. Lahann, *Journal of the American Chemical Society*, 2010, 132, 18023-18025.
30. R. Fishler, A. Artzy Schnirman, E. Peer, R. Wolchinsky, R. Brener, T. Waks, Z. Eshhar, Y. Reiter and U. Sivan, *Nano Lett*, 2012, 12, 4992-4996.
31. D. Wright, B. Rajalingam, J. M. Karp, S. Selvarasah, Y. B. Ling, J. Yeh, R. Langer, M. R. Dokmeci and A. Khademhosseini, *J Biomed Mater Res A*, 2008, 85, 530-538.
32. X. Ye and L. Qi, *Nano Today*, 2011, 6, 608-631.
33. A. Scheffel, N. Poulsen, S. Shian and N. Kroger, *Proceedings of the National Academy of Sciences of the United States of America*, 2011, 108, 3175-3180.
34. Chien H.W. and Tsai W.B., *Acta biomaterialia*, 2012, 8, 3678-3686.
35. C. Yu, J. W. Ma, J. N. Zhang, J. Lou, D. H. Wen and Q. L. Li, *ACS applied materials & interfaces*, 2014, 6, 8199-8207.
36. A. M. Ross and J. Lahann, *Journal of Polymer Science Part B-Polymer Physics*, 2013, 51, 775-794.
37. J. Berger, M. G. Holthaus, N. Pistillo, T. Roch, K. Rezwan and A. F. Lasagni, *Applied Surface Science*, 2011, 257, 3081-3087.
38. M. g. Holthaus, S. Twardy, J. Stolle, O. Riemer, L. Treccani, E. Brinksmeier and K. Rezwan, *Journal of Materials Processing Technology*, 2012, 212, 614-624.
39. D. M. Chun, J. O. Choi, C. S. Lee, I. Kanno, H. Kotera and S. H. Ahn, *International Journal of Precision Engineering and Manufacturing*, 2012, 13, 1107-1112.
40. K. Lin, J. Pan, Y. Chen, R. Cheng and X. Xu, *Journal of Hazardous Materials*, 2009, 161, 231-240.
41. L. Xia, Z. Zhang, L. Chen, W. Zhang, D. Zeng, X. Zhang, J. Chang and X. Jiang, *Eur Cell Mater*, 2011, 22, 68-82; discussion 83.
42. T. Roy, D. Choudhury, A. Bin Mamat and B. Pingguan Murphy, *Ceramics International*, 2014, 40, 2381-2388.
43. J. Tang, R. Peng and J. Ding, *Biomaterials*, 2010, 31, 2470-2476.
44. D. Chen, M. A. Harris, G. Rossini, C. R. Dunstan, S. L. Dallas, J. Q. Feng, G. R. Mundy and S. E. Harris, *Calcified tissue international*, 1997, 60, 283-290.
45. H. Mayer, H. Bertram, W. Lindenmaier, T. Korff, H. Weber and H. Weich, *Journal of Cellular Biochemistry*, 2005, 95, 827-839.
46. K. Lin, P. Liu, L. Wei, Z. Zou, W. Zhang, Y. Qian, Y. Shen and J. Chang, *Chemical Engineering Journal*, 2013, 222, 49-59.
47. A. F. Cipriano, N. De Howitt, S. C. Gott, C. Miller, M. P. Rao and H. Liu, *Journal of Biomedical Nanotechnology*, 2014, 10, 660-668.
48. J. G. Li, K. Zhang, P. Yang, W. Qin, G. C. Li, A. S. Zhao and N. Huang, *Colloids and Surfaces B-Biointerfaces*, 2013, 110, 199-207.
49. V. Hasirci and B. J. Pepe Mooney, *Nanomedicine*, 2012, 7, 1375-1389.
50. A. Klymov, L. Prodanov, E. Lamers, J. A. Jansen and X. F. Walboomers, *Biomaterials Science*, 2013, 1, 135-151.

**Graphical Abstract:**
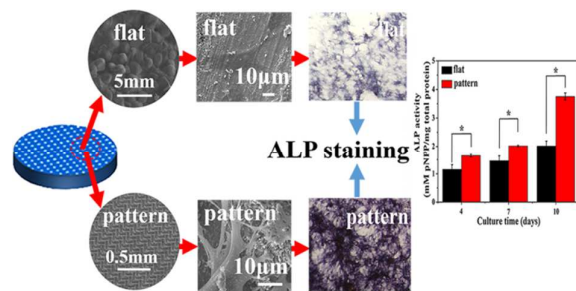


The HAp bioceramics with micropatterned surface significantly enhance cell responses.